JOURNAL OF MATERIALS SCIENCE 12 (1977) 11 (1976) 2258–2266

# X-ray topographic study of solid-state polymerized poly-[1, 2-bis-(*p* tolylsulphonyloxymethylene)-1-butene-3-inylene]

J. M. SCHULTZ*
*Institute für physikalische Chemie, Universität Mainz, Mainz, West Germany,*

Local extinction contrast effects have been observed in macroscopic polymer crystals, using Berg–Barrett X-ray topography. Results from as-polymerized crystals indicate that the crystals are perfect enough for defect regions to be imaged. As-polymerized crystals exhibited apparent defects lying along [0 2 1]. [0 1 0] slip traces in the (1 0 0) surface of a crystal were imaged; the slip system here appears to be consistent with $(h0l)$ $[\bar{l}0h]$, for $h, l \neq 0$ and [0 1 0] the chain direction.

## 1. Introduction

Under tensile loading, a semicrystalline polymer will typically undergo several stages of deformation. Over the first approximately 10% strain the deformation is elastic and localized in the amorphous regions which separate crystalline lamellae [1]. Over the next several tens of percent deformation, the crystalline units themselves can reversibly deform, giving rise to an elongation of the spherulites which they compose [2–4]. Beyond some strain level (which is of the order of 100%) the strain becomes irrecoverable [2, 5] and a tensile specimen may exhibit necking. Very large strains are associated with the breakdown of the original crystal units, at least into smaller blocks, and the formation of a new fibrillar system [6].

While the processes of spherulite and crystallite deformation have been observed, the micromechanisms of such deformation are as yet unknown. Most models of the deformation process ignore the details of the slip process within the crystals and are thus unable to predict the stress and temperature dependences. A computation by Peterson in 1966, however, suggested that dislocations could be generated spontaneously at sufficiently low strain-rates and could be entirely responsible for the large deformation of the crystalline entities [7]. However, although dislocations in thin polymer lamellar crystals have been observed through their Moiré fringes [8, 9], no direct evidence of their role in deformation is available. This lack of information is due largely to the very small size of the crystalline entities (see, e.g. [10]) and their sensitivity to damage in the electron microscope [11]. Direct study of the details of deformation processes in polymer crystals has, then, awaited the arrival of large, perfect polymer crystals.

Such large, relatively perfect crystals are now available and studies of deformation [12] and dislocation identification [13, 14] have begun. Large (several millimeters in any direction) single crystals can be routinely obtained through solid-state polymerization of a variety of monomers possessing triple bonds [15–19]. In these cases the monomer crystal acts as a template for the growing polymer chains, which propagate by the successive *in situ* linear attachment of monomer units. Schermann [13, 14] has observed apparent slip traces on poly-[1, 2-bis-(*p*-tolylsulphonyloxymethylene)-1-butene-3-inylene] (PT) crystals, the material of the present study. These crystals are

*Present address: Department of Chemical Engineering, University of Delaware, Newark, Delaware 19711, USA.

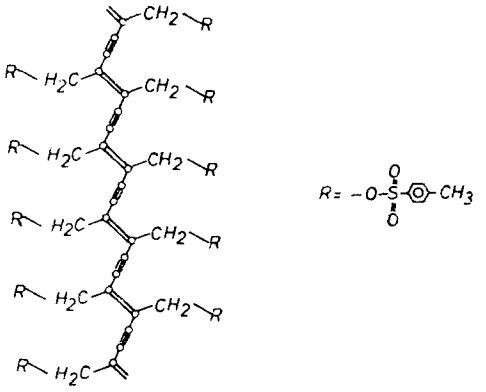

*Figure 1* Structure of the PT polymer chain.

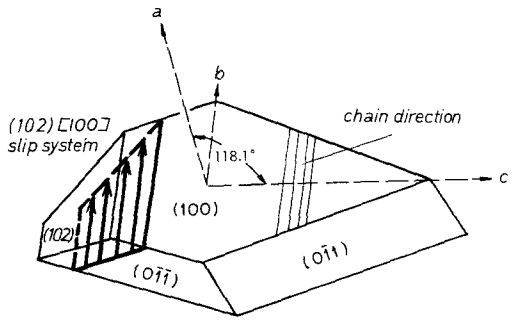


*Figure 2* Typical crystal of PT, showing crystallographic axes and possible slip system (1 0 2) [0 1 0].

monoclinic, with $a = 14.49$ Å, $b = 4.91$ Å, $c = 14.94$ Å, $\beta = 118.14°$ [20]. The chains are aligned along $b$. The chains themselves are composed of a carbon backbone with single, double and triple bonds and with large sidegroups, as shown in Fig. 1 [13, 14]. A typical crystal outline is sketched in Fig. 2, along with the slip system (1 0 2) [0 1 0] suggested by Schermann. Schermann has also observed apparent slip traces along [0 1 0], [$\bar{2}$ 2 1], and [2 2 $\bar{1}$] on the (1 0 2) external face. Of these, only [0 1 0] could be a direction of easy slip*. The other two traces would require that the slip plane cut across the polymer chains; chain kinks formed by such slip would require a high deformation energy. The other two slip systems – (1 0 2) [0 1 0] and the system with the trace [0 1 0] on (1 0 2) – would, on the other hand, be consistent with the general requirement that the slip plane lie parallel to the polymer chain [21] – the condition of no chain kinking.

Such crystals, large enough to exhibit well-developed slip traces, should also be large enough to yield direct X-ray topographic images of the lattice defects. The ability of these polymer crystals to do so would then depend only on the relative perfection of the crystals. X-ray topography, in general, consists of the microscopic examination of a diffraction spot, and is similar to dark-field electron microscopy. In the topographic method used here the elastically distorted region about a crystal defect yields a locally enhanced diffracted intensity, because primary extinction does not develop in these areas [22]. The image of a defect is thus really the image of its strain field. If the defects are quite close together, the strain fields will overlap and one will observe only a continuously very dark diffraction spot. This is the limiting condition of a "mosaic crystal" [23]. In metallic, ionic, or covalently-bonded crystals, one generally finds that a dislocation density above some $10^6$ lines/cm$^2$ will be unresolvable due to the overlap of the strain fields. The critical dislocation density for a polymer crystal should be lower, because the weak interchain molecular bonding should produce more extended strain fields. Thus, the perfection required for such studies is quite high.

The experimental apparatus is quite simple. X-rays from the spot focus of an X-ray tube are brought, at the Bragg angle $\theta$, onto a set of lattice planes in a single crystal. The diffracted beam is then recorded on a film placed approximately parallel to the primary beam and as close as possible to the specimen surface. This latter condition is important, as resolution decreases with distance from the specimen surface. This back-reflection geometry (termed the Berg–Barrett geometry [22, 24]) requires no special specimen size or thickness, in contrast to the transmission, or Lang [25] geometry. In the latter, a variety of defect imaging effects can be observed, depending on the specimen thickness and beam collimation and planarity [26]. Both methods are normally non-destructive and permit macroscopic driving forces (such as heat [27], deformation [28], or chemical attack [29]) to be applied between X-ray exposures. Further, since the stress field about a dislocation is anisotropic, its effect on the intensity of reflection from different crystal planes will

*It should be mentioned that the rounded appearance of the ⟨$\bar{2}$ 2 1⟩ bands may be more consistent with a kink band than with a slip trace.

vary. To an approximation (for an isotropic material) the intensity will vary as $\mathbf{S} \cdot \boldsymbol{b}$, where $\mathbf{S}$ is a unit vector normal to the diffracting plane and $\boldsymbol{b}$ the Burgers vector, scaled to unity [22]. Thus, ideally, one should be able to observe crystal dislocations (and other defects), determine their Burgers vectors and observe the effect of external variables on them. A review of the Berg–Barrett method and results has recently been given by Armstrong and Wu [30].

## 2. Experimental

Polymer crystals were obtained from Dr D. Batchelder at Queen Mary College, London, and from Dr W. Schermann and Professor G. Wegner at Universität Mainz. The synthesis and crystallization of the monomer is described by Wegner [15]. Polymerization was induced by heat-treatment (70° C in the case of the Mainz crystals). Crystals typically had the shape sketched in Fig. 2 and were several millimeters in each dimension.

The simple Berg–Barrett camera used here has been described in [28]. The crystal from Queen Mary College was examined at the University of Delaware, using Fe$K\alpha$ radiation from the spot focus of a General Electric CA7 X-ray tube driven at 35 kV and 15 mA. The Mainz crystals were examined, at Mainz, using Cu$K\alpha$ radiation from the spot focus of a Philips tube (Type PW 2103), driven at 30 kV and 30 mA. Exposure times were

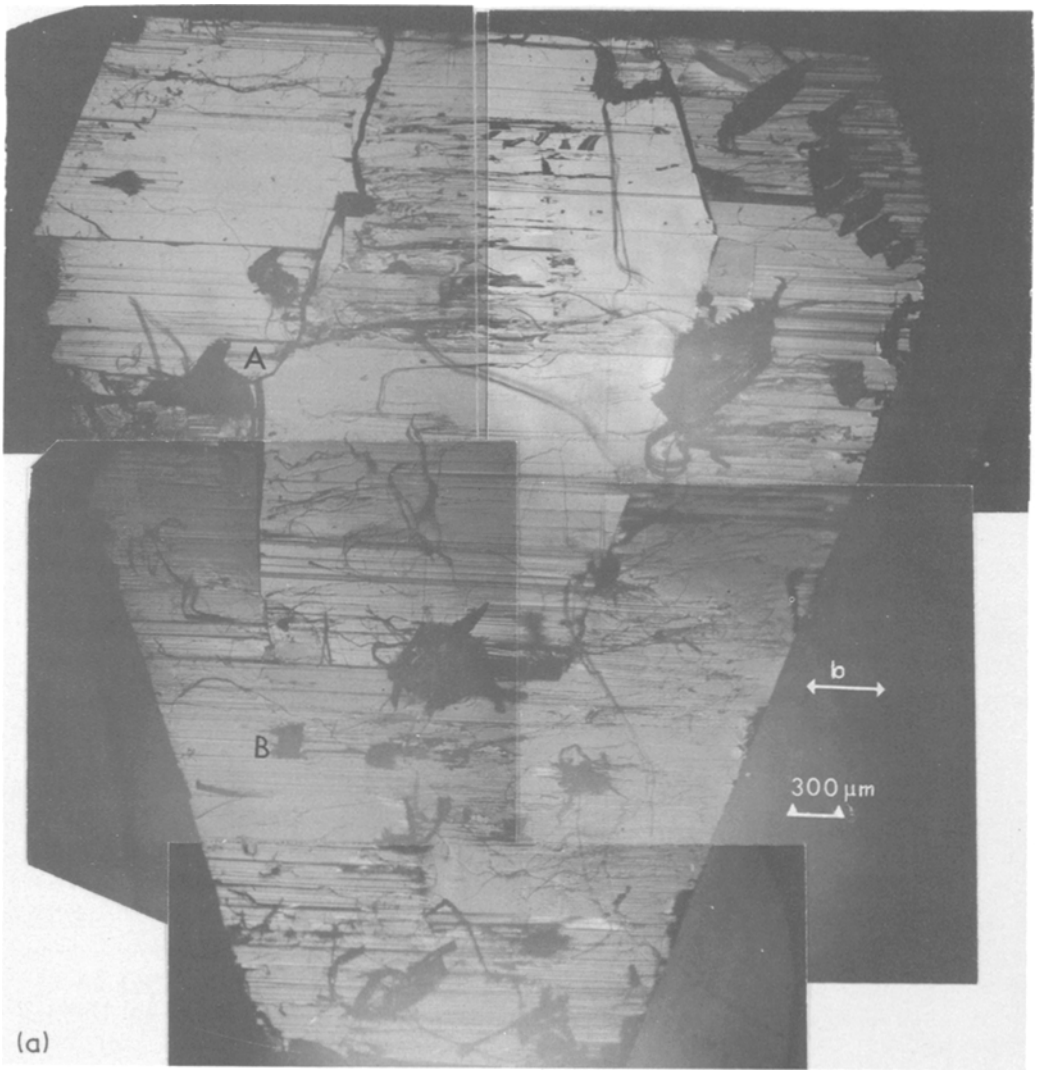


*Figure 3* PT crystal from Queen Mary College: (a) optical micrograph; (b) (2 0 1) topograph from (1 0 0) surface; (c) (7 0 0) topograph from (1 0 0) surface.

TABLE I Diffracting planes and angles, (1 0 0) surface

| Radiation | Bragg plane | Order of reflection | Entrant angle, $\epsilon$, degrees | Bragg angle, $\theta$, degrees |
|---|---|---|---|---|
| Cu$K\alpha$ | (1 0 0) | 2 | 7 | 7 |
| | (1 0 0) | 5 | 17 | 17 |
| | (3 0 1) | 6 | 13 | 27 |
| Fe$K\alpha$ | (1 0 0) | 4 | 18 | 18 |
| | (1 0 0) | 7 | 32 | 32 |
| | ($\bar{3}$ 0 1) | 8 | 15 | 34 |

typically of the order of 1 h, but were, in extreme cases, as long as 6 h. Kodak High Resolution Plate was used to record the diffraction spot.

These crystals exhibited numerous reflections, generally at small Bragg angles $\theta$. Several reflecting planes were used in this study. In Table I the diffraction conditions for several Bragg planes are listed, for cases in which observation is made through the broad (1 0 0) surface. It should be pointed out, however, that our apparatus did not permit accurate determination of the angles $\epsilon$ and $\theta$ (see Fig. 6); hence, the Bragg planes indicated in Table I are approximations, corresponding to low index planes broadly consistent with the observations. In addition, Berg–Barrett micrographs were made, for one crystal, from (0 1 1) and (1 0 2) surfaces. The diffracting planes used in these cases lay at angles below 21° (and usually much less) from the exposed surface. Finally, two transmission topographs have been made using Cu$K\alpha$ radiation. One topograph was from ($\bar{1}$ 0 2) and the other from approximately (0 1 2).

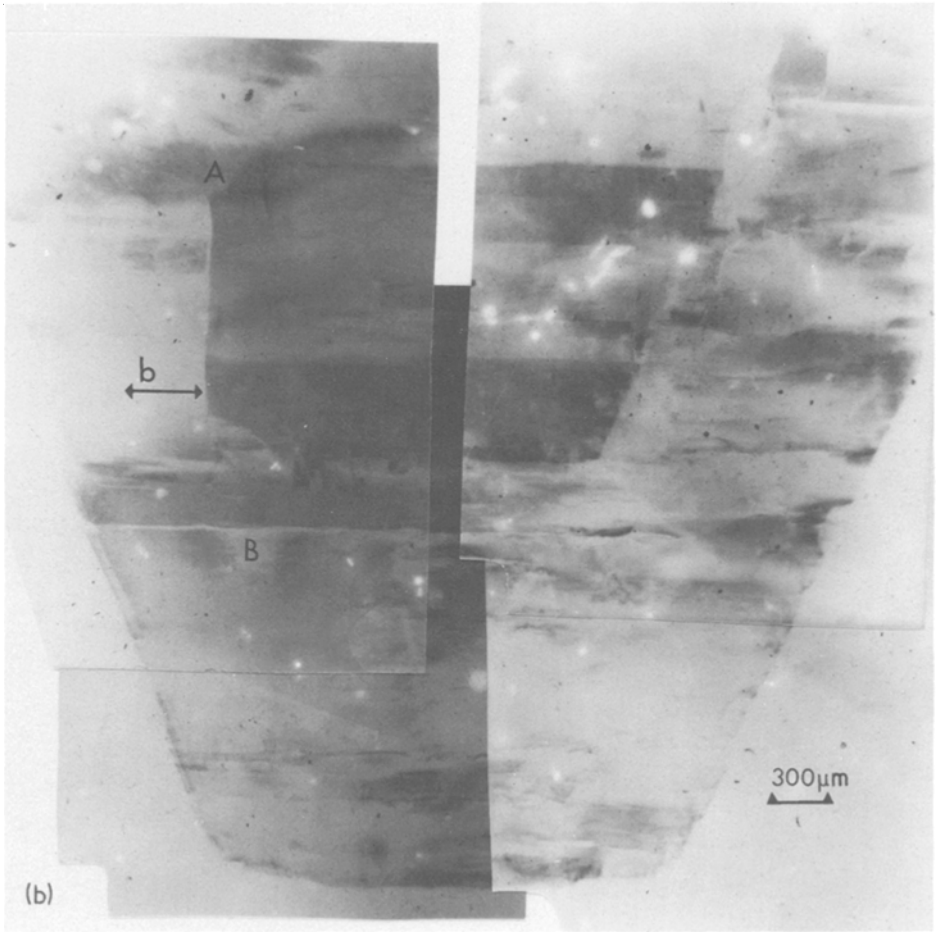


*Figure 3* continued.

## 3. Results

112 exposures have been made. The majority of these show at least local regions which exhibit extinction contrast. Most Bragg spots, however, indicate a good deal of lattice curvature, as indicated by broad intensity variations across the surface. Nevertheless, the perfection within any reflecting zone is apparently great enough to reveal local extinction effects.

A crystal from Queen Mary College (apparently rather carefully prepared) was studied using Fe$K\alpha$ radiation. Fig. 3 shows (a) an optical micrograph of the (1 0 0) surface, (b) a (2 0 1) topograph, and (c) a (7 0 0) topograph. In (c) the plane of the incident and diffracted rays contained the chain axis $b$; that is, the specimen was rotated 90° about $\mathbf{a}^*$ between (b) and (c). Regions on the three micrographs can be compared using the features A and B as fiducial marks. In (b) only the cleavage steps and other gross surface features, seen in the optical micrograph (a), can be observed. In (c) however, one can also observe regions of local extinction contrast (apparent defects), such as those at C and D. These regions are bounded by circular defects. An enlargement of the regions C and D is shown as Fig. 4. A network is to be observed within the circular border C, and a fine structure is also observed within the more or less elliptical regions D. It is possible that the circular

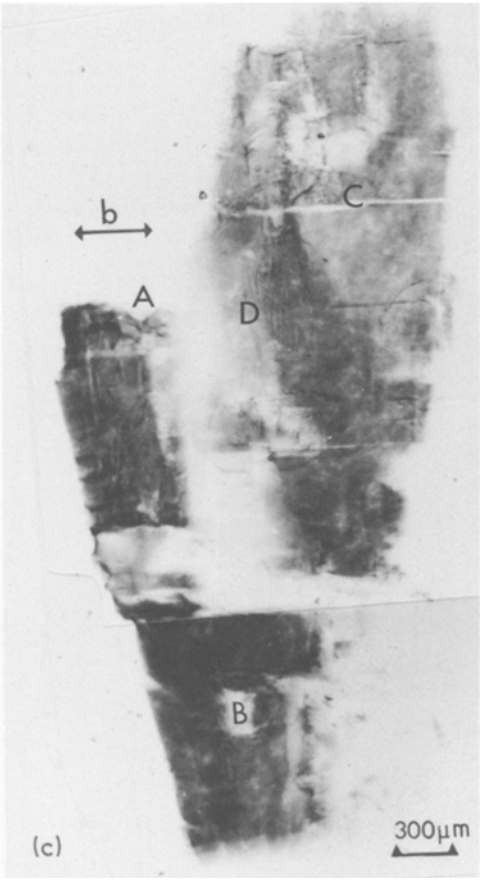


*Figure 3* continued.

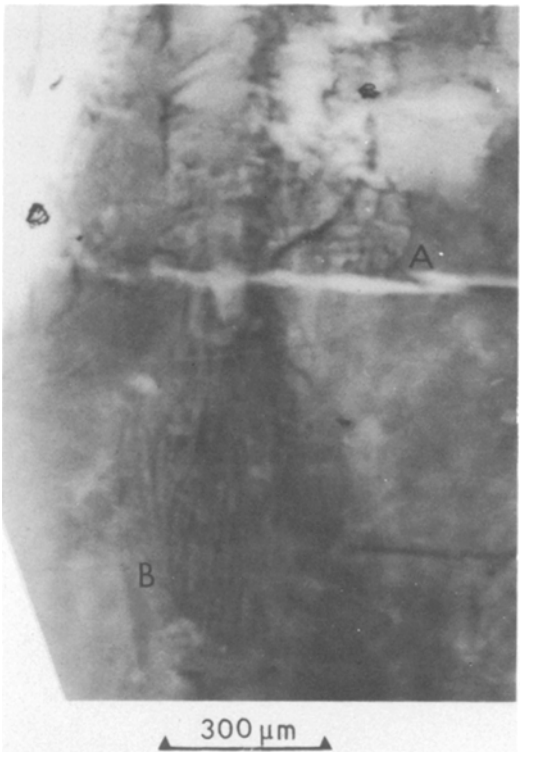


*Figure 4* Enlargement of portion of Fig. 3c.

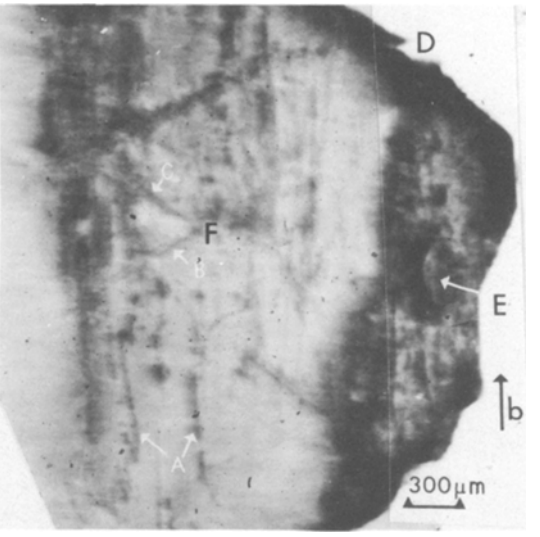


*Figure 5* X-ray topograph images of PT crystal from Mainz, 5 0 0 reflection, in geometry of Fig. 6.

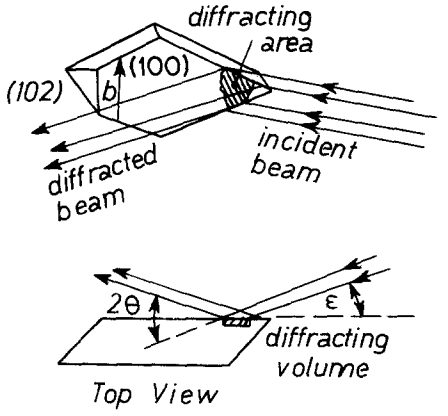


*Figure 6* Experimental geometry associated with topograph of Fig. 5.

or elliptical reflections denote dislocation rings formed with Burgers vectors not lying in (1 0 0). Only in this way could $\mathbf{g} \cdot \boldsymbol{b}$ be zero in $\bar{3}0\,1$ and be finite in $h\,0\,0$ reflections. These defects could have been formed to alleviate an epitaxy problem during polymerization. The networks within those domains would similarly form to alleviate polymerization strains.

Fig. 5 shows an enlargement of a portion of a diffraction spot from a particularly large and perfect PT crystal from Mainz. The experimental geometry for this topograph is sketched in Fig. 6.


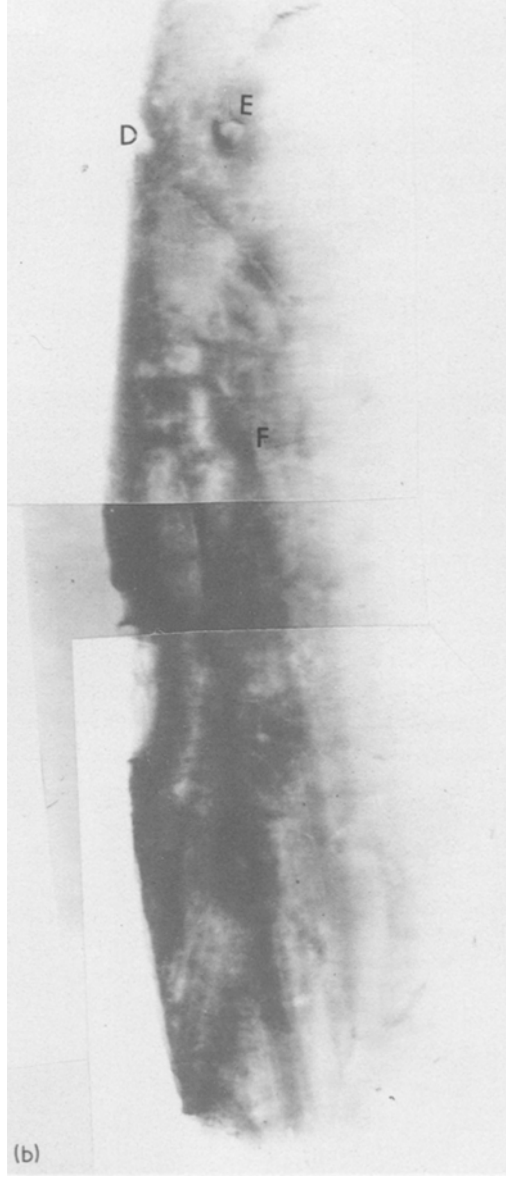


*Figure 7* 5 0 0 plane reflections from the crystal of Fig. 5.

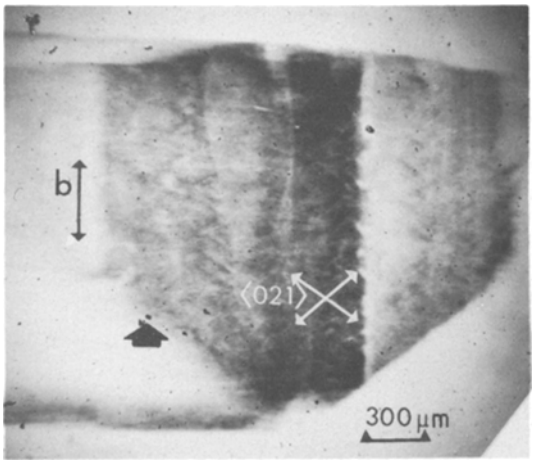


*Figure 8* PT crystal (from Mainz) showing high densities of defect images parallel to [0 2 1].

Here the incident and diffracted rays lie in the plane normal to ***b***, the polymer chain direction. In this topograph the angle $\epsilon$ between incident beam and (1 0 0) is ~7° and $2\theta$ is ~14°; this corresponds to 2 0 0 diffraction. Fig. 7 is from the same crystal surface, but with the crystal rotated 90° (clockwise and anticlockwise) about the normal to (1 0 0). That is, the plane of the incident and diffracted rays now lies parallel to ***b***. Fig. 7a and b are both basal plane (5 0 0) reflections. It is to be noted that in all our X-ray topographs the image is foreshortened by a factor of approximately one-half. The surface scars D and E and the line intersection F can be used to compare regions on the three micrographs. Many, but not all. of the features seen in Fig. 5 are also seen in Fig. 7. For instance, the lines B and C which intersect at F are prominent in all micrographs, as are other features which run in similar directions. Lines such as those meeting at F are not seen in the specimen surface

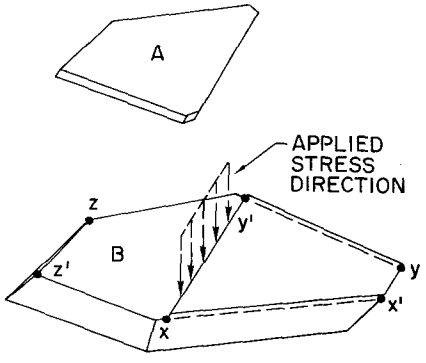


*Figure 9* Sketch of fracture geometry, specimen of Figs. 5 and 7.

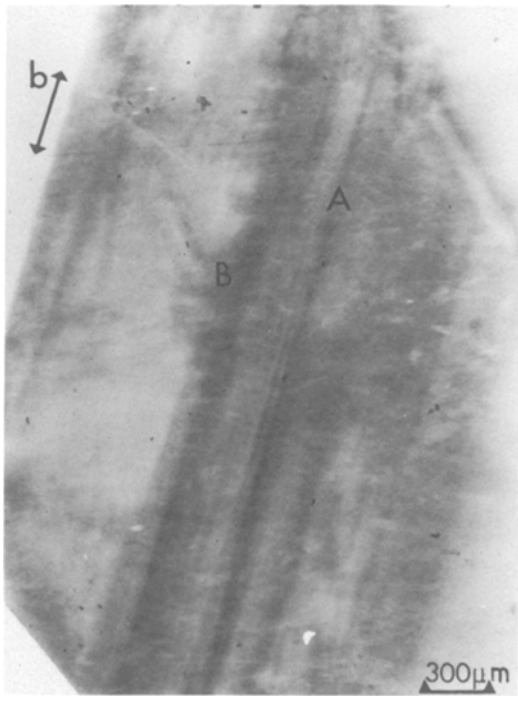


*Figure 10* (2 0 0) topograph of area near stress application, fragment B.

and, hence, cannot be a relief imagery. Indeed, surface relief images characteristically show either adjacent light and dark bands, or else appear dark in one view and light in the 180°-rotated exposure. Hence, these images probably manifest extinction contrast.

These lines and those seen parallel to them near the bottom of Fig. 7a and 7b run parallel to [0 2 1]. Extinction lines running parallel to [0 2 1] were a common feature of the Mainz PT crystals. Often a much greater density of lines was observed, as seen in Fig. 8. These lines cross the chain axis and indicate some sort of chain-bending defect. Most probably, such deformation would be produced during polymerization and may be a vestige of defects which existed in the monomer.

Segmented lines, such as those at A in Fig.5, do not appear in Fig. 7. It is at present not resolved whether these images reflect surface steps or arise from internal features.

A few attempts were made to observe crystals after mechanical deformation. Usually the crystal would fragment during the deformation process. The remaining pieces sometimes showed severe lattice curvature, making resolution untenable. However, enough regions of low enough strain

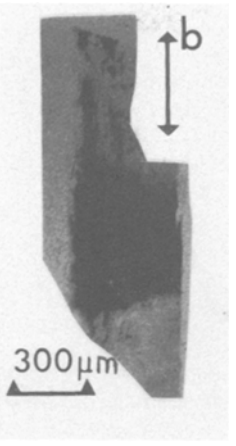


*Figure 11* Portion of (1 0 2) Lang (transmission) topograph of PT crystal from Mainz.

density exist to permit some inferences regarding deformation details.

The crystal of Fig. 5 and 7 was indented with a dull screwdriver, with the blade parallel to ***b***. The crystal broke as indicated in Fig. 9. The fragment A contains the region of Fig. 5. The large fragment B was then cleaved with a razor blade along the plane $xx'yy'$, to provide the new (1 0 0) surface $xx'yy'zz'$. Deformation features could be resolved in B, in the vicinity of the area where the stress was applied. Fig. 10 is a (2 0 0) topograph of this area. Apparent slip traces parallel to [0 1 0] are seen. In the original crystal surface, no such slip traces can be seen. Individual dislocations within the slip traces appear as black dots or short line segments. The slip plane for this system would be of the type ($h0l$), consistent with the condition that the slip plane contain the chain axis $b$.

A thin slice, cleaved parallel to the basal plane (and mechanically deformed somewhat by bending about ***b***) was observed in transmission. A portion of the (1 0 2) topograph of this crystal is shown in Fig. 11. Most of the field of view was uniformly blackened, but the traces of fine bands running parallel to ***b*** were seen at the sides of the black region. This observation is consistent with that of Fig. 10; that is, bending about $b$ is apparently accommodated by slip on some ($h0l$) plane.

## 4. Discussion

The relatively high perfection of the PT crystals is itself noteworthy. In most crystals, there could be observed at least a few regions in which the total lattice distortion was low enough for local extinction contrast to be resolvable. Considering the general lack of care in ensuring perfection during growth of the monomer crystals produced in Mainz and also considering the low intermolecular forces in these crystals, it is likely that the monomer crystals were relatively imperfect. In fact, preliminary investigation of monomer crystals produced in Mainz indicate defect densities bordering on or above our limits of resolution. Thus it appears that the "healing" of lattice defects and polymerization operate in parallel. Nevertheless, at least some of the defects in the monomer are apparently replicated in the polymer, as evidenced by the apparent chain-traversing defects observed.

The possible basal plane slip traces seen here in as-polymerized crystals are not entirely those observed by Schermann *et al.* [14]. The [0 1 0] and approximately [0 5 1]* traces seen by Schermann *et al.*, were not observed here, but rather an approximately [0 2 1] trace was seen. It is clear that additional work is needed in order to confirm the active slip systems in the monomer, and in the polymer.

## 5. Conclusion

Local extinction contrast images have been observed in PT crystals using Berg–Barrett X-ray topographs. It is conjectured that the perfection necessary for such results was produced simultaneously with polymerization.

As-polymerized crystals exhibited [0 2 1] defect lines in (1 0 0). Since such defects would require the permanent kinking of polymer chains, it is likely that the polymer crystal has replicated dislocations generated in the monomer. Deformed polymer crystals exhibited apparent $(h\,0\,l)$ $[\bar{l}\,0\,h]$ slip traces.

## Acknowledgements

This work was supported by the Deutsche Forschungsgemeinschaft and the National Science Foundation. The author is indebted to Dr David Batchelder, Dr Walter Schermann, and Professor Gerhard Wegner for the PT crystals and especially to Dr Schermann for long and patient discussions in the early stages of this work. Thanks are extended to Professor H. Ruppersberg and Ms C. Birkenheier for permission to use and help in using the Lang camera.

*This is given incorrectly as [0 1 5] in [14].

## References


1. W. E. KAUFMAN and J. M. SCHULTZ, *J. Mater. Sci.* 8 (1973) 41.
2. V. A. KARGIN and I. YU. TSAREVSKAYA, *Polymer Sci. USSR* 8 (1966) 1601.
3. P. M. GORBUNOV, *ibid* **11** (1969) 436.
4. J. L. WAY and J. R. ATKINSON, *J. Mater. Sci.* 6 (1971)
5. V. A. KARGIN, G. P. ANDRIANOVA, and G. G. KARDASH, *Polymer Sci. USSR* 9 (1967) 289.
6. A. PETERLIN and K. SAKUOKU, *Kolloid Z.* **212** (1966) 51; *J. Appl. Phys.* 38 (1967) 4152.
7. J. M. PETERSON, *ibid* **37** (1966) 4047.
8. V. F. HOLLAND, *ibid* **35** (1964) 1351.
9. K. ABE, M. MINOMI and M. TAKAYANAGI, *J. Macromol. Sci. Phys.* **4B** (1970) 87.
10. J. M. SCHULTZ, "Polymer Materials Science" (Prentice-Hall, Englewood Cliffs, New Jersey, 1974).
11. D. T. GRUBB, *J. Mater. Sci.* 9 (1974) 1715.
12. R. H. BAUGHMAN, H. GLEITER and N. SENDFELD, *J. Polymer Sci., Polymer Phys. Ed.* **13** (1975) 1871.
13. G. WEGNER and W. SCHERMANN, *Colloid and Polymer Sci.* **252** (1974) 655.
14. W. SCHERMANN, G. WEGNER, J. O. WILLIAMS and J.M. THOMAS, *J. Polymer Sci., Polymer Phys. Ed.* **13** (1975) 753.
15. G. WEGNER, *Makromol. Chem.* **145** (1971) 85.
16. *Idem, ibid* **154** (1972) 35.
17. J. KAISER, G. WEGNER and E. W. FISCHER, *Kolloid Z.* **250** (1972) 1158.
18. J.KIJI, J. KAISER, G. WEGNER and R. C. SCHULZ, *Polymer* **14** (1973) 433.
19. R. H. BAUGHMAN, *J. Polymer Sci., Polymer Phys. Ed.* **12** (1974) 1511.
20. D. KOBELT and E. F. PAULUS, *Acta Cryst.* **B30** (1973) 232.
21. H. D. KEITH and E. PASSAGLIA, *J. Res. Nat. Bur. Stan.* **68A** (1964) 513.
22. J. B. NEWKIRK, *Phys. Rev.* **110** (1958) 1465; *Trans. Amer. Inst. Min. (Metall.) Engs.* **215** (1959) 483.
23. C. G. DARWIN, *Phil. Mag.* **43** (1922) 800.
24. C. S. BARRETT, *Trans. Amer. Inst. Min. (Metall.) Engs.* **161** (1945) 15.
25. A. R. LANG, *J. Appl. Phys.* **30** (1959) 1748.
26. A. AUTHIER, in "Modern Diffraction and Imaging Techniques in Materials Science", edited by S. Amelinckx, R. Gevers, G. Remant and J. Van Landuyt (North-Holland, Amsterdam, 1970).
27. J. M. SCHULTZ and J. WASHBURN, *J. Appl. Phys.* **31** (1960) 1800.
28. J. M. SCHULTZ and R. W. ARMSTRONG, *Phil. Mag.* **10** (1964) 497.
29. R. W. ARMSTRONG and J. M. SCHULTZ, *Surface Sci.* **12** (1968) 19.
30. R. W. ARMSTRONG and C. C. WU, in "Microstructural Analysis: Tools and Techniques", edited by L. McCALL and W. M. MUELLER (Plenum, New York, 1973).


Received 10 February and accepted 2 April 1976.